Effective quantum state reconstruction using compressed sensing in NMR quantum computing

J. Yang,[1] S. Cong,[1,*] X. Liu,[2] Z. Li,[2] and K. Li[3]

[1]*Department of Automation, University of Science and Technology of China, Hefei 230027, People's Republic of China*

[2]*Department of Physics, University of Science and Technology of China, Hefei 230026, People's Republic of China*

[3]*Imperial College London, MRC Institute of Medical Sciences, London, W12 0NN, United Kingdom*

(Received 16 June 2017; published 1 November 2017)

Compressed sensing (CS) has been verified as an effective technique in the reconstruction of quantum state; however, it is still unknown if CS can reconstruct quantum states given the incomplete data measured by nuclear magnetic resonance (NMR). In this paper, we propose an effective NMR quantum state reconstruction method based on CS. Different from the conventional CS-based quantum state reconstruction, our method uses the actual observation data from NMR experiments rather than the data measured by the Pauli operators. We implement measurements on quantum states in practical NMR computing experiments and reconstruct states of two, three, and four qubits using fewer number of measurement settings, respectively. The proposed method is easy to implement and performs more efficiently with the increase of the system dimension size. The performance reveals both efficiency and accuracy, which provides an alternative for the quantum state reconstruction in practical NMR.

DOI: 10.1103/PhysRevA.96.052101

I. INTRODUCTION

Nuclear magnetic resonance (NMR) is one of the most promising physical methods to realize quantum computing, which has attracted tremendous interest in both the physics and information science community [1–4]. In practical NMR quantum computing experiments, the reconstruction of quantum states occupies an important position. Conventional quantum state tomography (QST) is a common method for NMR quantum state reconstruction [5–7], which requires fully informationally complete measurements of the quantum state to be reconstructed. For an n-qubit state ρ, the number of complete measurements is $d^2 = 4^n$. This number increases exponentially with n and makes the reconstruction work of the high-qubit NMR state become extremely difficult. In order to reduce the number of measurements, people sometimes use local quantum tomography [8] to reconstruct the states. However, local quantum tomography requires a sufficient amount of prior information before reconstructing, which does not have universal applicability. Therefore, the reconstruction of high-qubit NMR quantum states has great challenge.

Compressed sensing (CS) [9] has attracted a great interest as an effective approach of recovering sparse signals. This approach is now widely applied in many fields, such as image processing [10,11], wireless communication [12], nuclear magnetic resonance imaging (MRI) [13,14], NMR spectroscopy [15,16], and so on. CS also provides a new idea for the reconstruction of quantum states. One necessary condition of quantum compressed sensing used in QST is the density matrix of the quantum state should be low rank, that is, the rank r of the density matrix is much less than the dimension d of the Hilbert space: $r \ll d$. The theory of CS indicates that a low-rank-r density matrix can be reconstructed from $O(rd \log d)$ randomly sampled measurements [17]. To achieve such a reconstruction, one needs to solve an estimator of the convex optimization problem consisting of the sampled measurement data [18]. People can use different styles of convex optimization problems, such as the nuclear-norm minimization, trace minimization, and least-square (LS) minimization. The positivity constraint of the density matrix needs to be included in the optimization to ensure the effectiveness of the reconstruction [19]. Given the compressed number of samples and an appropriate optimization algorithm, the solution of the convex optimization problem with positivity constraint is the reconstruction of the quantum state. Several optimization algorithms have been used to solve the different optimization problems of the density matrices in quantum systems, such as LS, Dantzig, gradient projection, singular value thresholding, and so on [18,20,21]. Li and Cong first applied the alternating direction method of multipliers (ADMM) algorithm to QST and showed that the ADMM algorithm has better performance than the previous algorithms when considering the sparse noises [22,23]. Zheng *et al.* combined the fixed point idea and the ADMM algorithm and proposed the FP-ADMM algorithm, which improves further the calculation efficiency and the reconstruction accuracy [24].

By using CS, researchers obtained accurate quantum state reconstructions in some physical systems such as atomic spins [18], photons [25–27], and trapped ions [28,29]. However, it is still not clear if CS can reconstruct quantum states provided measurement data from NMR, because the measurements of NMR are obtained in a different way. In practical NMR computing experiments, the signal of each measurement is sampled in the time domain and then transferred into the frequency-domain spectrum. The spectrum contains a number of resonance peaks, and each peak is associated with an observable O_i of the system. The observables of the same spectrum constitute an NMR observable group, which can be measured simultaneously. When reconstructing an actual NMR state ρ based on CS, due to the particularity of practical NMR measurements, the observables are sampled in units of observable groups rather than individual observables, which is different from the sampling method in conventional quantum compressed sensing [30–32].

*scong@ustc.edu.cn

In this paper, we show that CS can also be applied to the NMR quantum state reconstruction, and one can directly use the observable groups. We theoretically prove that CS can be applied to the reconstruction of actual NMR quantum states and give the detailed reconstruction steps, which combine CS and the characteristics of the practical NMR measurement. FP-ADMM is used as the optimization algorithm to solve the nuclear-norm optimization problem. We experimentally verify the efficiency of the proposed method by the reconstruction of actual NMR states with two, three, and four qubits and analyze the effects of factors on the reconstruction performance.

The structure of this paper is as follows. In Sec. II, after a brief introduction to the practical NMR measurement method, the CS theory, and the FP-ADMM algorithm, we prove our reconstruction method and give specific steps of the method. In Sec. III, the experimental reconstruction results are shown. We perform reconstruction of actual two, three, and four qubits NMR states, respectively, and analyze the reconstruction performance through contrast experiments. The conclusion of this paper is given in Sec. IV.

II. QUANTUM STATE RECONSTRUCTION BASED ON COMPRESSED SENSING AND ACTUAL NMR OBSERVATION DATA

As an indirect measurement process, the system to be measured in NMR is an n-qubit quantum state consisting of nuclear spins in the sample solution under a constant z-direction magnetic field B_0. There is a magnetic moment of the nuclear spins in the magnetic field, whose direction is the same as B_0 and the magnitude is proportional to the angular momentum of the spin. The external control field is a radio frequency (rf) pulse magnetic field on the $x-y$ plane. When applying an rf pulse consisting of a plurality of resonant frequencies to the sample solution, the nuclear spins absorb the energy of the rf pulse, and the angle between the magnetic moment and B_0 changes, leading to a Larmor precession. There is an induction coil winding on the surface of the sample solution, and the nuclear precession results in a free induction decay current signal $s(t)$ in the induction coil: $s(t)=\sum_i \mathbf{M}_0 e^{i\Omega_i t}e^{-t/T_2}$, where t stands for time, Ω_i denotes the resonant frequencies, and i is the flag, $\mathbf{M}_0$ is the value of fixed rf field magnetization intensity vector, and T_2 represents the transverse relaxation time. $S(\omega)$ is a frequency-domain spectrum which is obtained from the Fourier transform of $s(t)$: $S(\omega)=\int_0^\infty s(t)e^{-i\omega t}dt = A(\omega)+iB(\omega)$, where ω stands for the frequency, $A(\omega)=\sum_i \mathbf{M}_0 {T_2}^{-1}/(\omega-\Omega_i)^2+{T_2}^{-2}$ and $B(\omega)=\sum_i \mathbf{M}_0(\omega-\Omega_i)/(\omega-\Omega_i)^2+{T_2}^{-2}$ are the real and imaginary parts of $S(\omega)$, respectively. The spectrums of $A(\omega)$ and $B(\omega)$ near the resonant frequency Ω_i are resonance peaks, with the peaks of $A(\omega)$ being absorption peaks and those of $B(\omega)$ being symmetric dispersion peaks.

When measuring an n-qubit quantum state ρ whose dimension is $d=2^n$, each resonance peak in $S(\omega)$ corresponds to an observable O_i, and the observation value of O_i is proportional to the area of the signals in the corresponding peak of $A(\omega)$:

$$\langle O_i\rangle = \frac{1}{\mathbf{P_0}}\int_{\Omega_i-\Delta\omega}^{\Omega_i+\Delta\omega} A(\omega)d\omega, \tag{1}$$

where $\mathbf{P_0}$ is the scaling factor which can be determined by the peak's area of the eigenstate in the same sample solution, and $\Delta\omega$ is a fixed range value, which ensures all signals of the selected format are included in the frequency range $[\Omega_i-\Delta\omega,\Omega_i+\Delta\omega]$.

As the spectrum $S(\omega)$ contains d resonance peaks, the observation data of the corresponding d observables are obtained simultaneously in one NMR measurement. Such d observables constitute an NMR observable group, defined as $\{O_j^k\}=\{O_1^k,O_2^k,\ldots,O_d^k\}$, where $j=1,2,\ldots,d$ and $k=1,2,\ldots,v$ is the serial number of the group. Here v denotes the total number of the observable groups which is determined by the composition of the experimental sample and the actual measurement scheme. For example, O_j^k represents the jth observable in the kth group and is also expressed in the subscript form as $O_j^k=O_{kj}$. $\{O_i\}$ $(i=1,2,\ldots,vd)$ is the set of all the observables. In practical NMR experiments, people design a measurement scheme of v different NMR observable groups to measure the complete observables of ρ, with some inevitably repetitive or linearly related observables in different groups, meaning that the total observables of $\{O_i\}$ are overcomplete for ρ.

In order to implement the conventional QST in NMR, people need to perform the following transformation to the observables $\{O_i\}$: based on the d observables in each group $\{O_j^k\}$, people transform $\{O_j^k\}$ into a set of measurement operators $\{M_j^k\}=\{M_1^k,M_2^k,\ldots,M_d^k\}$ according to the transformation formula $M_j^k=\sum_i^{2^{n-1}} h_{ij}O_j^k$, where M_j^k is an n-qubit Pauli operator that is the tensor product of Pauli matrices $\{I,X,Y,Z\}=\{\left(\begin{smallmatrix}1&0\\0&1\end{smallmatrix}\right),\left(\begin{smallmatrix}0&1\\1&0\end{smallmatrix}\right),\left(\begin{smallmatrix}0&-i\\i&0\end{smallmatrix}\right),\left(\begin{smallmatrix}1&0\\0&-1\end{smallmatrix}\right)\}$, and h_{ij} is one of the elements in the transformation matrix $\mathbf{H}$ of $\{O_j^k\}$ and $\{M_j^k\}$. Each column of $\mathbf{H}$ represents a linear transformation from $\{O_j^k\}$ to one operator of $\{M_j^k\}$. The corresponding observation values $\{\langle O_j^k\rangle\}$ can be transformed to the measured values $\{\langle M_j^k\rangle\}$ in the same way. Since the observables of $\{O_i\}$ are overcomplete, there are repetitions of the measurement operators in different $\{M_j^k\}$. People need to remove all the repetitions from $\{M_j^k\}$ to get a complete set of measurement operators $\{M_m\}$ $(m=1,2,\ldots,d^2)$, then one can calculate the reconstructed density matrix $\hat{\rho}$ of the state ρ with $\{M_m\}$ and $\{\langle M_m\rangle\}$: $\hat{\rho}=\frac{1}{2^n}\sum_{m=1}^{4^n}(\langle M_m\rangle M_m)$. However, as the number of qubits n increases, the number of measurement operators required for QST d^2 increases exponentially, and the corresponding actual NMR measurement becomes extremely cumbersome.

Here we propose an effective reconstruction method of the actual NMR quantum states based on CS, in which we directly use observable groups $\{O_j^k\}$ but not the transformed Pauli measurement operators $\{M_m\}$. The reconstruction process can be described as to solve the following convex optimization problem of nuclear-norm minimization:

$$\min \|\rho\|_*, \quad \text{such that } \mathbf{y}=\mathbf{A}\,\mathrm{vec}(\rho), \tag{2}$$

where $\|\rho\|_*$ represents the nuclear norm of ρ, which equals the sum of singular values; $\mathrm{vec}(\cdot)$ represents the transformation from a matrix to a vector by stacking the matrix's columns in order on top of one another. The sampling matrix $\mathbf{A}$ is the matrix form of all the sampled observables and the sampling

vector $\mathbf{y}$ is the vector form of the corresponding observation values.

Considering the measurement method in NMR experiments, it is not practical to use the transformed measurement operators $\{M_m\}$ as the observables because each M_m is obtained by means of much more observables in groups in practical NMR experiments. Thus we directly use the randomly sampled observable groups $\{O_j^k\}$ and the corresponding actual observation values $\{\langle O_j^k\rangle\}$ in the quantum compressed sensing. Because the observables and observation values are sampled in groups, here we defined a new sampling rate as

$$\eta_g = g/v, \tag{3}$$

where g is the number of the sampled groups and v is the total number of groups. It is worth mentioning that η_g is different from the general sampling rate $\eta_m = m/d^2$, where m and d^2 represent the sampled number and total number of the measurement operators $\{M_m\}$, respectively, and $\eta_g, \eta_m \in [0,1]$.

Without loss of generality, assuming that the randomly sampled serial numbers are from 1 to g, then $\mathbf{A}$ and $\mathbf{y}$ in NMR can be written as

$$\mathbf{A} = \begin{pmatrix} \mathrm{vec}\left(\{O_j^1\}\right)^T \\ \mathrm{vec}\left(\{O_j^2\}\right)^T \\ \vdots \\ \mathrm{vec}\left(\{O_j^g\}\right)^T \end{pmatrix} \Big/ \sqrt{d} \tag{4}$$

and

$$\mathbf{y} = \left(\{\langle O_j^1\rangle\}, \{\langle O_j^2\rangle\}, \ldots, \{\langle O_j^g\rangle\}\right)^T, \tag{5}$$

where $\mathrm{vec}(\{O_j^k\})^T$ represents the transformation from the d observables of $\{O_j^k\}$ to d horizontal vectors arranged in vertical order:

$$\mathrm{vec}\left(\{O_j^k\}\right)^T = \begin{pmatrix} \mathrm{vec}\left(O_1^k\right)^T \\ \mathrm{vec}\left(O_2^k\right)^T \\ \vdots \\ \mathrm{vec}\left(O_d^k\right)^T \end{pmatrix},$$

and $\mathbf{y}$ is the vector of the observation values corresponding to the observables of $\mathbf{A}$. In this case, the optimization problem (2) is an equation group composed of $g \times d$ equations. It should be noted that, since the total observables are overcomplete, there may be some repeating equations in (2), but this repetition does not affect the solution of (2).

Candes *et al.* proved that, if the sampling matrix $\mathbf{A}$ satisfies the rank restricted isometry property (RIP) [33], the convex optimization problem (2) has a unique optimal solution equaling the true density matrix [34]. The sampling matrix $\mathbf{A}$ consisting of $O(rd\log^2 d)$ randomly sampled Pauli measurement operators satisfies rank RIP with very high probability [20]. Since the transformation between the operators of $\{O_j^k\}$ and $\{M_j^k\}$ is linear, if the sampling matrix $\mathbf{A}_M$ consisting of g different Pauli measurement operator groups $\{M_j^k\}$ satisfies rank RIP, then the sampling matrix $\mathbf{A}_O$ that consists of corresponding g observable groups $\{O_j^k\}$ also satisfies rank RIP. This means, in theory, our method sampling the observable groups $\{O_j^k\}$ is applicable to the reconstruction of actual NMR quantum state ρ.

A mathematical principle in quantum mechanics is that the eigenvalues of a physical quantum system must be nonnegative, which is called the positivity constraint. People must consider the positivity constraint when reconstructing the state by solving the optimization problem (2) [19,25], and the positivity constraint can be mathematically formulated as the following form: $\rho \geqslant 0$. Moreover, there are inevitable noises in the measurement data $\mathbf{y}$ due to the system and measurement error in practical NMR experiments. The experimental noises are more likely to be reflected by sparse outlier entries in ρ rather than Gaussian noise [24]. Using a sparse matrix S to represent the noises, the optimization problem (2) becomes

$$\begin{aligned} &\min_{\rho,S} \|\rho\|_* + \lambda\|S\|_1 + I_C(\rho), \\ &\text{such that } \|\mathbf{y} - \mathbf{A}\,\mathrm{vec}(\rho + S)\|_2^2 \leqslant \varepsilon, \quad \rho \geqslant 0, \end{aligned} \tag{6}$$

where λ is a compromise factor $\lambda > 0$, $\|\cdot\|_1$ is the (1,1) norm, and $I_C(\rho)$ is the indictor function on a convex set C,

$$I_C(\rho) = \begin{cases} \infty & \text{if } \rho^\dagger = \rho,\ \rho \geqslant 0, \\ 0 & \text{otherwise.} \end{cases}$$

The function of $I_C(\rho)$ is projecting ρ into a positive semidefinite Hermitian matrix. ε stands for the error-level parameter of the reconstruction.

Conversional QST optimization algorithms such as LS and maximum likelihood can barely handle S, because the low-rank property will be significantly affected by these small portions of outliers. In this paper, we use the FP-ADMM algorithm proposed by Zheng *et al.* [24] to solve the optimization problem (6). FP-ADMM algorithm is a combination of the fixed point idea and ADMM algorithm, which can handle both normal errors and sparse outliers S in the density matrix. By leveraging the fixed point equation approach to avoid the matrix inverse operation, FP-ADMM can effectively reduce the computational complexity. The iterative steps of the FP-ADMM algorithm are as follows:

$$\begin{aligned} \rho_1^{k+1} &= D_{\delta\frac{1}{\mu}}\left\{\mathrm{mat}\left[(I - \delta\mathbf{A}^\dagger\mathbf{A})\mathrm{vec}\left(\rho_1^k\right) \right.\right. \\ &\qquad \left.\left. + \delta\mathbf{A}^\dagger\left(\mathbf{y} - \mathbf{A}\,\mathrm{vec}(S^k) - \frac{Y^k}{\mu}\right)\right]\right\}, \\ \rho^{k+1} &= \frac{1}{2}\left[\rho_1^{k+1} + \left(\rho_1^{k+1}\right)^\dagger\right], \\ S^{k+1} &= S_{\delta\frac{\lambda}{\mu}}\left\{\mathrm{mat}\left[(I - \delta\mathbf{A}^\dagger\mathbf{A})\mathrm{vec}(S^k) \right.\right. \\ &\qquad \left.\left. + \delta\mathbf{A}^\dagger\left(\mathbf{y} - \mathbf{A}\,\mathrm{vec}(\rho^{k+1}) - \frac{Y^k}{\mu}\right)\right]\right\} \\ Y^{k+1} &= Y^k + \mu[\mathbf{A}\,\mathrm{vec}(\rho^{k+1} + S^{k+1}) - \mathbf{y}], \end{aligned} \tag{7}$$

where S is a sparse matrix representing interference terms, which is updated alternatively with ρ in the iterative process, $\mathrm{mat}(\cdot)$ is the inverse operator of $\mathrm{mat}(\cdot)$, and $D_\lambda(\mathbf{X})$ is the singular value contraction operator defined as $D_\lambda(\mathbf{X}) = US_\lambda(S)V^T$, where USV^T is the singular value decomposition of $\mathbf{X}$. In every iteration, the singular values of the density matrix are pushed to be positive to satisfy the positivity constraint [35].

$S_\lambda(\mathbf{X})$ is the soft threshold defined as

$$[S_\lambda(\mathbf{X})]_{ij} = \begin{cases} x_{ij} - \lambda, & \text{if } x_{ij} > \lambda, \\ x_{ij} + \lambda, & \text{if } x_{ij} < \lambda, \\ 0, & \text{otherwise.} \end{cases}$$

$Y \in R^m$ is the Lagrange multiplier and $\delta \in [0, +\infty]$ is the iterative step size, $\lambda, \mu > 0$. In the reconstruction experiments of this paper, the parameters of FP-ADMM algorithm are selected as follows: $\delta = 1$, $\lambda = 1/\sqrt{d}$, and $\mu = 0.5/\|\mathbf{y}\|_F$ [22]; the initial values of ρ, S, and Y are taken as zero matrices. The error-level parameter ε should be set according to the amount of noise in the measurement data $\mathbf{y}$ [29,30], since a too small ε may cause the optimization problem to be infeasible, while a too big ε will reduce the precision of the reconstruction. In this paper, the error-level parameter is set as $\varepsilon = 10^{-7}\|y\|_F$ and the stopping criterion is $\|y - \mathbf{A}\,\mathrm{vec}(\rho^k + \mathbf{S}^k)\|_F < \varepsilon$ or the number of iterations $k > 30$.

In general, the process of reconstructing NMR quantum states with the method proposed can be summarized as follows: randomly sample a certain number of $\{O_j^k\}$ and $\{\langle O_j^k\rangle\}$, construct the convex optimization problem (6) with the sampled $\{O_j^k\}$ and $\{\langle O_j^k\rangle\}$, and solve (6) with the FP-ADMM algorithm. The final optimal solution $\hat{\rho}$ is the reconstruction result of the state ρ.

The fidelity is used as the performance index of state reconstruction and is defined as f:

$$f = \mathrm{Tr}(\hat{\rho}\rho^\dagger)/\sqrt{\mathrm{Tr}(\hat{\rho}^2)\mathrm{Tr}(\rho^2)}, \tag{8}$$

where $\hat{\rho}$ and ρ represent the experimentally reconstructed density matrix and the corresponding ideal density matrix, respectively, and $f \in [0,1]$.

III. EXPERIMENTAL STATES RECONSTRUCTION IN NMR AND ANALYSIS

We implement practical NMR experiments to reconstruct the states of $n = 2,3,4$ qubits, respectively, in order to examine the reduction performance of the number of measurements of our method. The experiments are carried out on a Bruker AV-400 spectrometer (9.4 T) at a room temperature of 303.0 K [8]. The physical systems of $n = 2,3,4$ qubits states are ^{13}C-labeled chloroform ($CHCL_3$) dissolved in deuterated acetone, Diethyl-fluoromalonate ($C_7H_{11}FO_4$) dissolved in ^{2}H-labeled chloroform, and iodotrifiuoroethylene (C_2F_3I) dissolved in d-chloroform, respectively. One ^{1}H and one ^{13}C are used for the first and second qubit of $n = 2$, and one ^{1}H, ^{13}C, and ^{19}F are used for the first, second, and third qubit of $n = 3$. For $n = 4$, one ^{13}C is labeled as the first qubit, and $^{19}F_1$, $^{19}F_2$, and $^{19}F_3$ as the second, third, and fourth qubits, respectively. The systems are first prepared into pseudopure states (PPS) using the line selective-transition method [17] in the experiment device. Then, by adjusting the pulse rf, the pseudopure states are manipulated into the target quantum state $|\psi_2\rangle$, $|\psi_3\rangle$, and $|\psi_4\rangle$ [7,8].

The state vectors associated with these three kinds of states are

$$|\psi_2\rangle = |00\rangle, \tag{9}$$

$$|\psi_3\rangle = \frac{4}{5}|000\rangle - \frac{3}{5}|001\rangle, \tag{10}$$

$$|\psi_4\rangle = \frac{1}{\sqrt{2}}(|0101\rangle + |1010\rangle), \tag{11}$$

in which $|0\rangle = \binom{1}{0}$ and $|1\rangle = \binom{0}{1}$ represent the ground state and the excited state of the nucleus, respectively. $|\psi_2\rangle$ is an eigenstate, and $|\psi_3\rangle$ and $|\psi_4\rangle$ are superposition states.

Let $\rho_2 = |\psi_2\rangle\langle\psi_2|$, $\rho_3 = |\psi_3\rangle\langle\psi_3|$, and $\rho_4 = |\psi_4\rangle\langle\psi_4|$ be the corresponding density matrices of $|\psi_2\rangle$, $|\psi_3\rangle$, and $|\psi_4\rangle$. In order to accurately reconstruct ρ_2, ρ_3, and ρ_4, the states $|\psi_2\rangle$, $|\psi_3\rangle$, and $|\psi_4\rangle$ need to be prepared and observed repeatedly for the complete observation data. In practical NMR experiments, the total number of observable groups used in our method are $v_2 = 6$, $v_3 = 16$, and $v_4 = 44$ for $n = 2,3,4$, respectively. The corresponding numbers of observables in each group are $d_2 = 2^2 = 4$, $d_3 = 2^3 = 8$, and $d_4 = 2^4 = 16$. Thus the total number of observables O_i for $|\psi_2\rangle$, $|\psi_3\rangle$, and $|\psi_4\rangle$ are $6 \times 4 = 24$, $16 \times 8 = 128$, and $44 \times 16 = 704$, respectively. After doing the transformation, the same number of measurement operators M_m are obtained, in which most of the obtained measurement operators are repeated. The complete d^2 measurement operators $\{M_m\}$ are selected from the obtained operators by removing all the repetitions, with d^2 being 16, 64, and 256 for $n = 2,3,4$, respectively. This means that when using m randomly sampled measurement operators $\{M_m\}$ to reconstruct the state, the actual number of operators needed to be measured in NMR is much greater than m, and many measurement results are not fully utilized. That's why we use the directly measured observable groups $\{O_j^k\}$ and the corresponding actual observation values $\{\langle O_j^k\rangle\}$ as the sampled measurement data in the proposed method, which also improves the efficiency by omitting the transformation process.

The ability of reconstructing quantum states using less sampling rate is very significant. We do the experiments to demonstrate this ability in different cases. We carry out the experiments for three scenarios by using two kinds of optimization algorithms and using two kinds of sampling matrices for the comparisons: randomly sampling from the observable groups $\{O_j^k\}$ by solving (A) optimization problem (6) using FP-ADMM algorithm and (B) non-negative least-square minimization: $\min_\rho \|\mathbf{A}\,\mathrm{vec}(\rho) - \mathbf{y}\|_2$ such that $\mathrm{Tr}\rho = 1, \rho \geqslant 0$ [19]; (C) randomly sampling from the Pauli measurement operators M_m by solving optimization problem (6) using FP-ADMM algorithm. It should be noted that in scenario (C) the measurement values of all M_m are obtained before doing the reconstruction experiments, because M_m cannot be sampled separately in practical NMR experiments as described in Sec. II. The sampling rate η_g in (3) is usually used to demonstrate the reduction performance of the number of the observable groups $\{O_j^k\}$, and $\eta_m = m/d^2$ is used for the measurement operators $\{M_m\}$. The performance index of state reconstruction is the fidelity in (7). Under each sampling rate, we reconstruct each state 100 times and average over

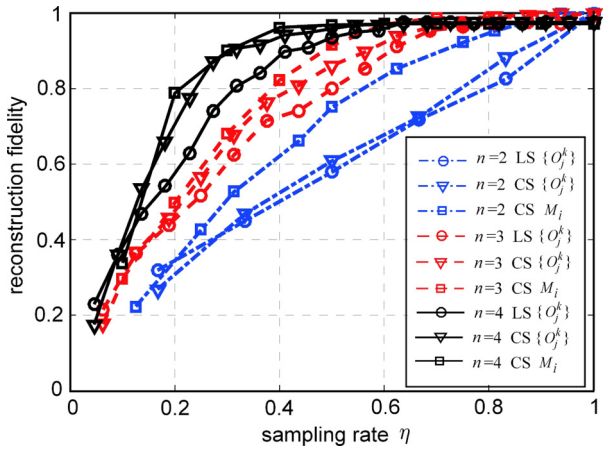

FIG. 1. Experimental results of reconstruction fidelities of ρ_2, ρ_3, and ρ_4 with different sampling rates in three different cases. The blue dot-dash line, red dashed line, and black solid line correspond to ρ_2, ρ_3, and ρ_4, and the triangle, circle, and square mark correspond to the cases of (A), (B), and (C), respectively. For cases (A) and (B), the incremental step of sampling rates are selected as $\Delta\eta_g = 1/6$, $1/16$, and $1/22$ of ρ_2, ρ_3, and ρ_4, respectively, and for case (C) the incremental step of sampling rate is fixed as $\Delta\eta_m = 0.1$.

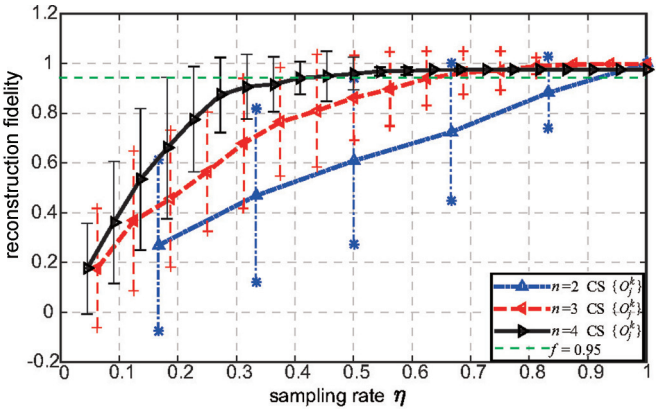

FIG. 2. Reconstruction average fidelity f_{avg} and mean-square error ζ at different sampling rates using QST-FP-ADMM. The blue dot-dash line with the inverted triangle, the red dash line with the left triangle, and the black solid line with the right triangle correspond to ρ_2, ρ_3, and ρ_4, respectively, while the star, plus, and dash symbols represent the corresponding error bars. The green dash line represents the reconstruction fidelity $f = 0.95$. The length of the error bar represents the mean-square error of the 100 experimental reconstruction fidelities.

the resulting fidelities as the final average fidelity f_{avg}. The experimental results of reconstruction fidelities of ρ_2, ρ_3, and ρ_4 with different sampling rates in three cases are shown in Fig. 1, which shows the reconstruction fidelities of two kinds of estimators consisting of the sampled observable groups $\{O_j^k\}$: (A) Eq. (6) of nuclear-norm minimization with FP-ADMM algorithm and (B) the non-negative least-square minimization, and the fidelities of two kinds of sampling matrices: (A) $\{O_j^k\}$ and (C) $\{M_m\}$ using compressed estimator (6) and FP-ADMM algorithm.

It can be seen from Fig. 1 that for the two kinds of sampling matrices $\{O_j^k\}$ and $\{M_m\}$, the reconstruction fidelity of $\{O_j^k\}$ becomes close to that of $\{M_m\}$ as the qubit number n increases for 2 to 4, and shows almost the same performance when $n = 4$. This experimental result indicates the sampling method of NMR proposed in this paper performs more and more efficiently with the increase of the system dimension size, which is more suitable for the reconstruction of high-qubit quantum states in NMR. Under the same observable groups $\{O_j^k\}$, because the sparse matrix of noise S is considered and optimized in the state reconstruction, the state reconstruction fidelities obtained by the FP-ADMM algorithm illustrate more accuracy than those of the LS algorithm without such a consideration. The experiment shows that, when $n \geqslant 3$, the proposed method can obtain high reconstruction fidelity with much less measurement data than the fully informationally complete measurement.

The mean-square error not only reflects the degree of discretization of the fidelities, but also responds to success probability of reconstruction at the corresponding sampling rate. We also do the experiments to study the mean-square error of the fidelity at the different sampling rates of the proposed method by solving (6) with sampling matrices $\{O_j^k\}$ using compressed FP-ADMM algorithm (referred to as QST-FP-ADMM). Here we use ζ to represent the value of mean-square error. In the experiments, we choose $f \geqslant 0.95$ as the criterion that the reconstruction is successful. When the average fidelity f_{avg} is near 0.95, the smaller of ζ, the more concentrated the fidelity distribution, and the higher the success probability of reconstruction, and vice versa. The reconstruction average fidelity f_{avg} and mean-square error ζ at different sampling rates using QST-FP-ADMM are shown in Fig. 2, which shows that the mean-square error ζ decreases with the increase of qubit number at the same sampling rate, e.g., the mean-square errors are $\zeta = 0.33$, 0.17, and 0.07 of $n = 2$, 3, and 4 with $\eta_g = 0.5$. ζ also tends to decrease with the increase of η_g at the same qubit number.

We set the mean-square error $\zeta \leqslant 0.1$ to get a sufficiently high success probability of reconstruction (the probability that $f \geqslant 0.95$). The least sampling rates for $\zeta \leqslant 0.1$ of $n = 2$, 3, and 4 are $\eta_g = 1$, 0.75, and 0.5, with the mean-square errors being $\zeta = 0$, 0.08, and 0.07, respectively. The least sampling rates are decreasing with the increase of qubit number. The average fidelities of reconstruction at these sampling rates are $f_{\text{avg}} = 1.0$, 0.97, and 0.96 and the corresponding success probabilities of reconstruction are 100%, 92%, and 97%. The experimental results show that we can carry out high-probability reconstruction of the quantum states in NMR with rather low sampling rates using the proposed method, especially for high-qubit quantum states.

The experimental reconstruction results of ρ_2, ρ_3, and ρ_4 by QST-LS and QST-FP-ADMM are shown in Fig. 3, and the reconstruction fidelities of Fig. 3 are shown in Table I.

TABLE I. Reconstruction fidelities of Fig. 3.

Fidelity	ρ_2	ρ_3	ρ_4
QST-LS	0.9942	0.9838	0.9606
QST-FP-ADMM	0.9999	0.9896	0.9679

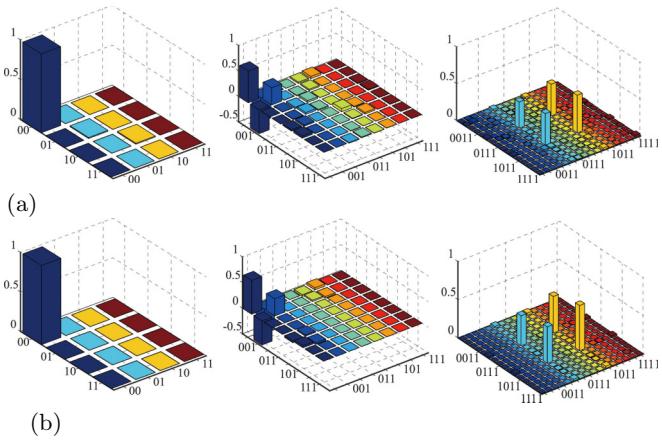

FIG. 3. Experimental results of reconstructed density matrices of ρ_2, ρ_3, and ρ_4. (a) The reconstruction by QST-LS with the sampling rate $\eta_m = 1$ and (b) the reconstruction by QST-FP-ADMM with the sampling rates $\eta_{g2} = 1.0$, $\eta_{g3} = 0.75$, and $\eta_{g4} = 0.50$. The three histograms from left to right in (a) and (b) correspond to the reconstructed density matrices of ρ_2, ρ_3, and ρ_4, respectively. Only the real parts of the reconstructed density matrices are given and the imaginary parts are ignored, because the imaginary parts of the elements in the ideal density matrices ρ_2, ρ_3, and ρ_4 are all zero.

In order to ensure a sufficiently high success probability of reconstruction, according to the experimental results of Fig. 2, we choose the sampling rates of ρ_2, ρ_3, and ρ_4 as $\eta_{g2} = 1.0, \eta_{g3} = 0.75$, and $\eta_{g4} = 0.50$, with the corresponding numbers of the sampled groups being $g_2 = 6$, $g_3 = 12$, and $g_4 = 22$.

The experimental results show that our method can reconstruct the actual NMR quantum states more accurately and effectively with only a small amount of observation data directly. The method proposed in this paper is the optimal reconstruction method under the existing conditions and can instruct the reconstructions of high-qubit quantum states in NMR.

IV. CONCLUSION

In this paper, we first reconstructed actual NMR quantum states via compressed sensing. We also proposed an effective NMR quantum state reconstruction method based on CS and gave a detailed derivation of the method in both theoretical and experimental aspects. The observation data is directly used in our method so as to save the transformation process of QST, which effectively enhances the efficiency of the state reconstruction in practical NMR experiments. We validated our method with actual measurement data of different qubit states and analyzed the effect of different factors on the reconstruction performance. The reconstruction performance reveals both efficiency and accuracy with the increase of system dimension size. The method proposed in this paper is both feasible in implementation and accurate in reconstruction and can greatly reduce the number of measurements required, which provides a protocol for the state reconstruction with higher qubits in practical NMR computing experiments.

ACKNOWLEDGMENT

This work was supported by the National Natural Science Foundation of China (Grant No. 61573330).

[1] J. A. Jones and M. Mosca, J. Chem. Phys. **109**, 1648 (1998).
[2] I. L. Chuang, L. M. K. Vandersypen, X. Zhou, D. W. Leung, and S. Lloyd, Nature (London) **393**, 143 (1998).
[3] L. M. K. Vandersypen, M. Steffen, G. Breyta, C. S. Yannoni, M. H. Sherwood, and I. L. Chuang, Nature (London) **414**, 883 (2001).
[4] C. Negrevergne, T. S. Mahesh, C. A. Ryan, M. Ditty, F. Cyr-Racine, W. Power, N. Boulant, T. Havel, D. G. Cory, and R. Laflamme, Phys. Rev. Lett. **96**, 170501 (2006).
[5] G. L. Long, H. Y. Yan, Y. S. Li, C. C. Tu, J. X. Tao, H. M. Chen, M. L. Liu, X. Zhang, J. Luo, L. Xiao, and X. Z. Zeng, Phys. Lett. A **286**, 121 (2001).
[6] J. S. Lee, Phys. Lett. A **305**, 349 (2002).
[7] Z. Li, M. H. Yung, H. Chen, D. Lu, J. D. Whitfield, X. Peng, A. Aspuru-Guzik, and J. Du, Sci. Rep. **1**, 88 (2010).
[8] J. Pan, Y. Cao, X. Yao, Z. Li, C. Ju, H. Chen, X. Peng, S. Kais, and J. Du, Phys. Rev. A **89**, 022313 (2014).
[9] E. J. Cands, J. Romberg, and T. Tao, IEEE Trans. Inf. Theory **52**, 489 (2006).
[10] N. Eslahi and A. Aghagolzadeh, IEEE Trans. Image Process. **25**, 3126 (2016).
[11] P. Sen and S. Darabi, IEEE Trans. Vis. Comput. Graph. **17**, 487 (2011).
[12] S. Stanković, I. Orović, and L. Stanković, Signal Process. **104**, 43 (2014).
[13] M. Lustig, D. Donoho, and J. M. Pauly, Magn. Reson. Med. **58**, 1182 (2007).
[14] M. L. Maguire, S. Geethanath, C. A. Lygate, V. D. Kodibagkar, and J. E. Schneider, J. Cardiovasc. Magn. Reson. **17**, 45 (2015).
[15] X. Andrade, J. N. Sanders, and A. Aspuru-Guzik, Proc. Natl. Acad. Sci. USA **109**, 13928 (2012).
[16] D. J. Holland, M. J. Bostock, L. F. Gladden, and D. Nietlispach, Angew. Chem. Int. Ed. **50**, 6548 (2011).
[17] X. Peng, X. Zhu, X. Fang, M. Feng, K. Gao, X. Yang, and M. Liu, Chem. Phys. Lett. **340**, 509 (2001).
[18] A. Smith, C. A. Riofrío, B. E. Anderson, H. Sosa-Martinez, I. H. Deutsch, and P. S. Jessen, Phys. Rev. A **87**, 030102 (2013).
[19] A. Kalev, R. L. Kosut, and I. H. Deutsch, npj Quantum Inf. **1**, 15018 (2015).
[20] Y. K. Liu, Adv. Neural Inf. Process. Syst. **24**, 1638 (2011).
[21] J. Zhang, K. Li, S. Cong, and H. Wang, Signal Process. **139**, 136 (2017).
[22] K. Li and S. Cong, IFAC Proc. **47**, 6878 (2014).
[23] K. Li, K. Zheng, J. Yang, S. Cong, X. Liu, and Z. Li, Quantum Inf. Process. (2017), doi: 10.1007/s11128-017-1720-x.
[24] K. Zheng, K. Li, and S. Cong, Sci. Rep. **6**, 38497 (2016).
[25] D. Gross, Y. K. Liu, S. T. Flammia, S. Becker, and J. Eisert, Phys. Rev. Lett. **105**, 150401 (2010).

[26] A. Shabani, R. L. Kosut, M. Mohseni, H. Rabitz, M. A. Broome, M. P. Almeida, A. Fedrizzi, and A. G. White, Phys. Rev. Lett. **106**, 100401 (2011).
[27] W. T. Liu, T. Zhang, J. Y. Liu, P. X. Chen, and J. M. Yuan, Phys. Rev. Lett. **108**, 170403 (2012).
[28] C. Schwemmer, G. Tóth, A. Niggebaum, T. Moroder, D. Gross, O. Gühne, and H. Weinfurter, Phys. Rev. Lett. **113**, 040503 (2014).
[29] C. A. Riofrío, D. Gross, S. T. Flammia, T. Monz, D. Nigg, R. Blatt, and J. Eisert, Nat. Commun. **8**, 15305 (2017).
[30] S. T. Flammia, D. Gross, Y. K. Liu, and J. Eisert, New J. Phys. **14**, 095022 (2012).
[31] T. Heinosaari, L. Mazzarella, and M. M. Wolf, Commun. Math. Phys. **318**, 355 (2013).
[32] C. J. Mioss, R. von Borries, M. Argaez, L. Velzquez, C. Quintero, and C. M. Potes, IEEE Trans. Signal Process. **57**, 2424 (2009).
[33] E. J. Candes and T. Tao, IEEE Trans. Inf. Theory **51**, 4203 (2005).
[34] E. J. Candes, C. R. Math. **346**, 589 (2008).
[35] K. Li, J. Zhang, and S. Cong, Phys. Rev. A **96**, 012334 (2017).